

Supporting Information for

**Tuning Crystalline Ordering by Annealing and Additives to
Study its Effect on Exciton Diffusion in a
Polyalkylthiophene Copolymer**

Mithun Chowdhury,^{a,†,‡} Muhammad T. Sajjad,^{a,†} Victoria Savikhin,^b Noémie Hergué,^c Karina B. Sutija,^a Stefan D. Oosterhout,^b Michael F. Toney,^b Philippe Dubois,^{c,††} Arvydas Ruseckas^a and Ifor D. W. Samuel^{a,}*

^aOrganic Semiconductor Centre, SUPA, School of Physics and Astronomy,
University of St. Andrews, North Haugh, St. Andrews, KY16 9SS, UK

^bStanford Synchrotron Radiation Lightsource, Menlo Park, CA 94025, USA

^cLaboratory of Polymeric and Composite Materials, University de Mons, Mons,
Belgium

Correspondence: idws@st-andrews.ac.uk (I. D. W. S.)

[‡]Present Address: Department of Chemical and Biological Engineering,
Princeton University, Princeton, NJ 08544, USA

^{††}Present Address: MRT Department, Luxembourg Institute of Science and
Technology - LIST, Belvaux, Luxembourg

[‡]M.C and M. T. S contributed equally to this work.

GIXS analysis to determine relative degrees of crystallinity

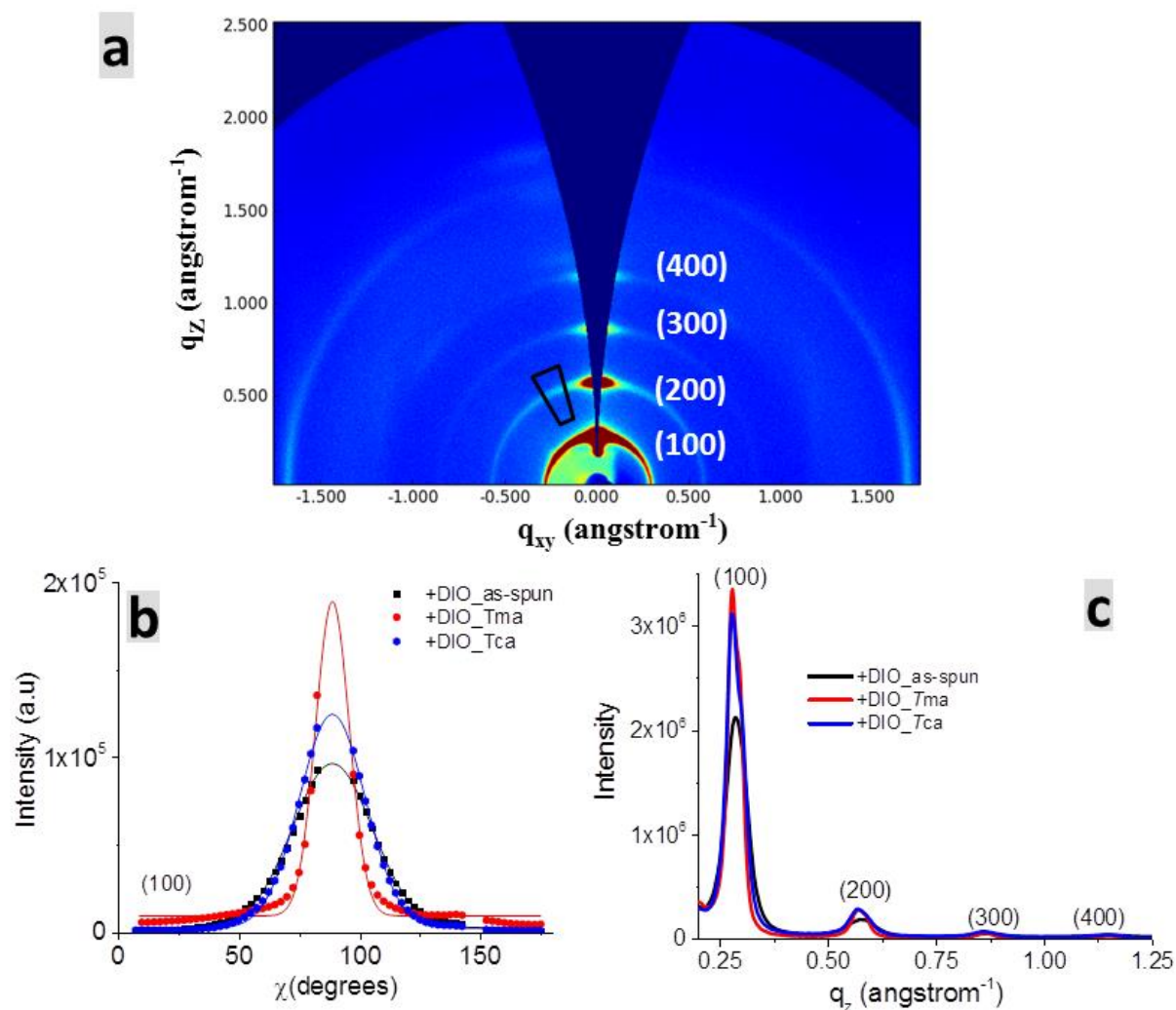


Figure S1: (a) Grazing incidence X-Ray scattering (GIXS) q_z - q_{xy} area image of P3HT-co-P3DDT (with 4% DIO), showing each (h00) peak. Further approximate pole figure (b) is constructed by values of integrated intensities found from the each cake slices in Q, with varying χ (c) Scattering intensities along q_z -direction for as-spun, melt annealed and thermally annealed film (along with additive 4% DIO).

Peaks in q for each χ slice were fitted to get rid of background; further area vs χ plot (approximate pole figure) was made using fitted peak areas. Then the relative degree of crystallinity (rDoC) is calculated by integrating the collected intensity over all χ . Such as for the (100) peak at $q = 0.28 \text{ \AA}^{-1}$ with q -range = $\pm 0.1 \text{ \AA}^{-1}$ and χ -range = 2.5° to 177.5° (**Figure S1b**). Because of the geometry of grazing-incidence diffraction, these approximate pole figures (**Figure S1b**) do not probe crystallites with their (100) direction oriented within a few degrees of the substrate normal, [J.L. Baker et al., *Langmuir* 26, 9146 (2010)], so a Gaussian fit is used to extrapolate the missing data within $\chi = 85^\circ$ to 95° (**Figure S1b**). Intensities are multiplied by a geometrical correction factor of $\text{Cos}(\chi)$ during integration [J. Rivnay *et al.*, *Chem. Rev.* 112, 5488 (2012)].

To calculate the average crystallite size, we fit each (h00) peak (e.g., **Figure S2c**) to a Gaussian function. We then fit the full width half max (fwhm) of each peak as a function of h (order of diffraction) squared using a linear fit. The slope of such a fit is related to the non-uniform strain of the crystallite, while the intercept is inversely proportional to the average crystallite size according to **equation S1** (Williamson-Hall analysis):

$$L_c = \frac{2\pi K}{b} \quad (\text{S1})$$

Here L_c is the crystallite size, K is a constant and assumed here to be ~ 1 , and b is the intercept extracted from the linear fit described above. **Table 1** summarizes data obtained on crystallite sizes from above analysis.

Comparison between P3DDT and P3HT-co-P3DDT

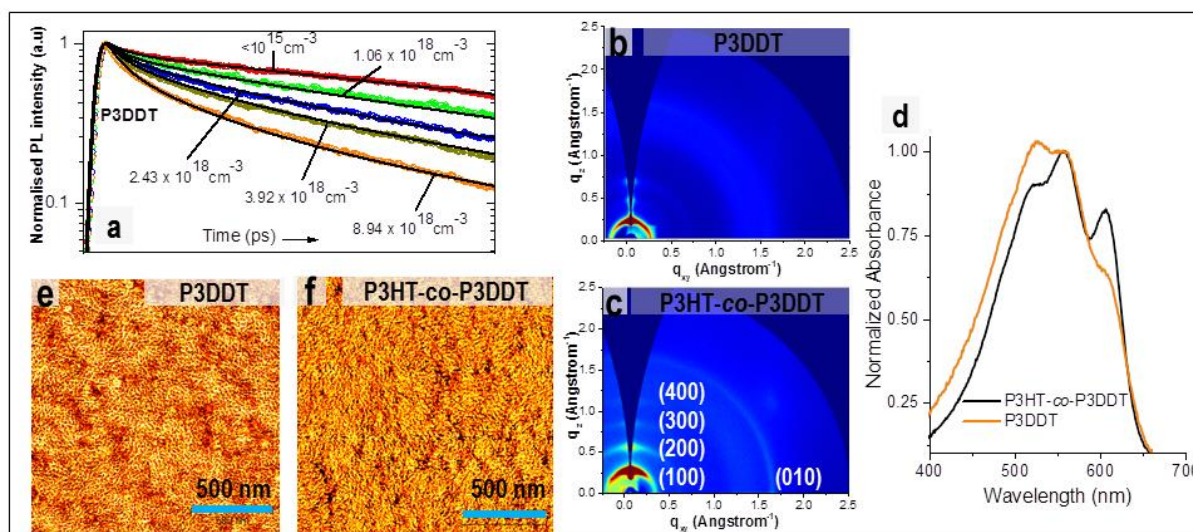


Figure S2. Fluorescence decays (a), grazing incidence X-Ray scattering (GIXS) q_z - q_{xy} 2D-area images (b) and AFM phase image (e) and absorption spectrum (d) of as-spun P3DDT film (thickness ca. 100 nm) shown in comparison to P3HT-co-P3DDT film. Scale bars in each AFM image correspond to 500 nm.

GIXS revealed more pronounced ($h00$) diffraction peaks and smaller d (100) -spacing in the copolymer P3HT-co-P3DDT (2.24 nm) in comparison to homopolymer P3DDT (2.52 nm). AFM phase images for both polymers showed percolated network of lamellar nanofibrils with relatively finer mesh for P3DDT (**Figure S2e-f**). The exciton diffusion coefficients measured by exciton-exciton annihilation was also higher in copolymer P3HT-co-P3DDT film ($1.2 \times 10^{-3} \text{ cm}^2 \text{ s}^{-1}$) as compared to homopolymer P3DDT ($0.65 \times 10^{-3} \text{ cm}^2 \text{ s}^{-1}$).

Fluorescence decays measured at different excitation densities

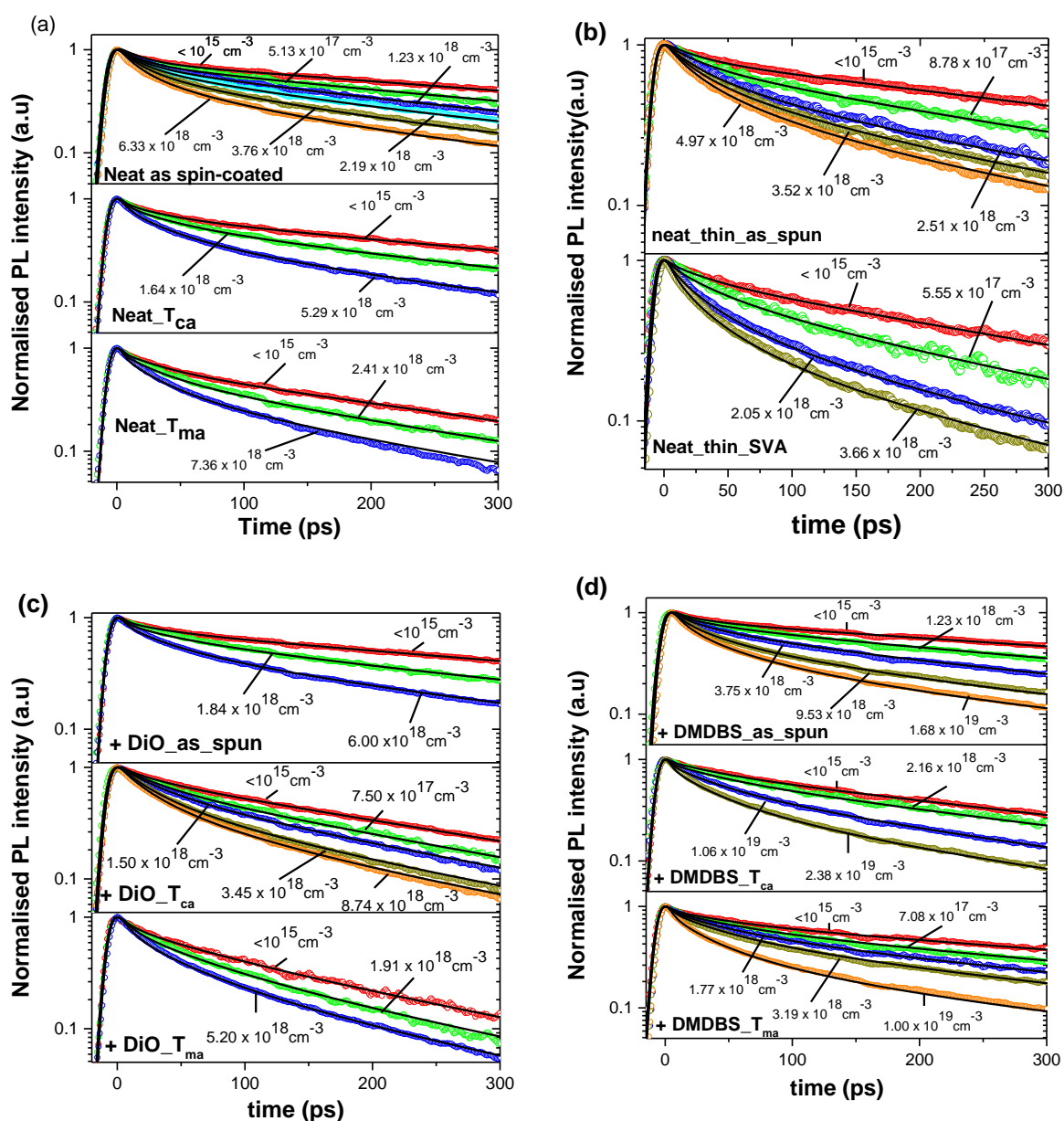


Figure S3: Fluorescence decays at different initial exciton densities in P3HT-co-P3DDT films spin-coated from neat solution and with solvent additives (DIO or DMDBS). T_{ca} indicates thermal annealing and T_{ma} melt annealing. The analysis was performed following the procedure described in the main manuscript (section 2.1). The time-dependent annihilation rate constant $\gamma(t)$ obtained from the fits for all samples is given in **Figure 2**.

Exciton diffusion length

We consider that the exciton diffusion coefficient, D , is the most useful quantity for developing structure-property relations for exciton diffusion because it is a single quantity. Diffusion length is more complicated because it depends on both diffusion coefficient and lifetime. We determined the one-dimensional exciton diffusion length (L_D) and plotted it against rDoC, exciton bandwidth (W), and the ratio of rDoC to exciton bandwidth (W) in **Figure S4**. L_D shows no clear correlation with rDoC or exciton bandwidth (**Figure S4a-c**). This suggests that exciton diffusion length does not relate directly to film crystallinity or conjugation length and depends on other variables including lifetime. For all films the estimated exciton diffusion length is smaller than the crystallite size except for the solvent-vapour annealed film where both are about 10 nm (Figure S5 in Supporting Information). It is possible that exciton diffusion length in this film is limited by crystallite size.

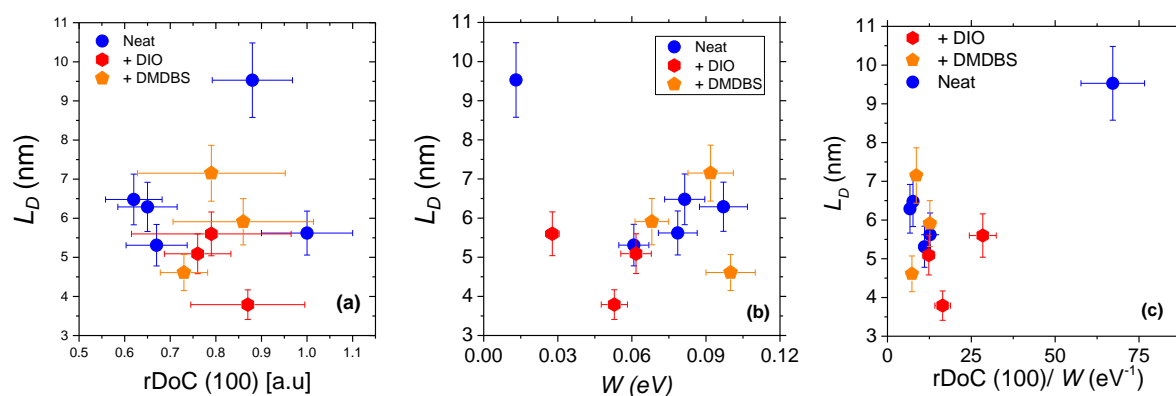


Figure S4: Dependence of one-dimensional exciton diffusion length L_D in P3HT-*co*-P3DDT films on a relative degree of crystallinity rDoC(100) (a); free exciton bandwidth W (b); and on the ratio of rDoC(100) and W (c). Films were spin-coated from neat solutions or with additives as indicated in the legend. Data points at $L_D = 9.5$ nm correspond to the solvent-vapour annealed thin film.

In **Figure S5**, we plotted the exciton diffusion coefficient (D) and length (L_D) against the crystallite size and found weak correlation between them.

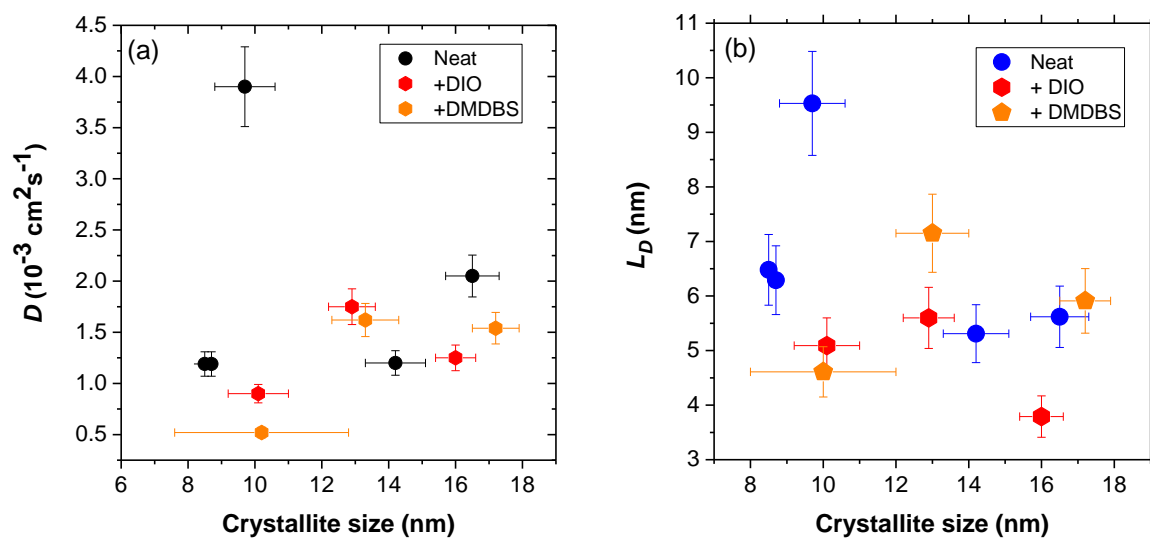


Figure S5: Dependence of exciton diffusion coefficient (a) and exciton diffusion length (b) in P3HT-co-P3DDT films on crystallite size.

AFM height topography

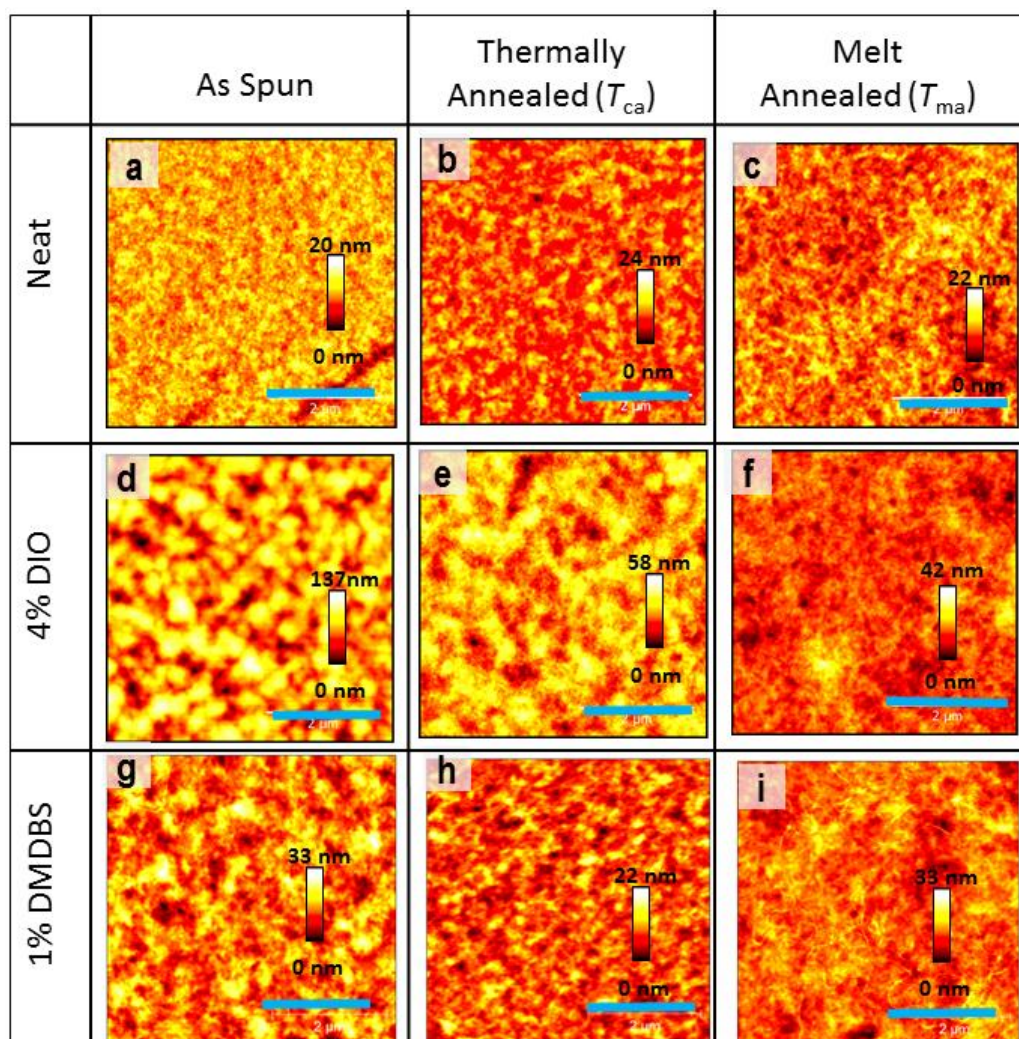


Figure S6: Atomic force microscopy (AFM) height (topography) images of as-spun (left column: a, d, g), thermally annealed (middle column: b, e, h) and melt annealed (right column: c, f, i) spin-coated films (ca. 100 nm thickness) of P3HT-*co*-P3DDT. Top row represents neat as-spun films, whereas, middle and bottom rows are with additives 4% DIO and 1% DMDBS respectively. Possible presence of trapped DIO led to structured surface with high roughness (d, R_a : ca. 16.5 nm) in comparison to a similar film without any additives (a, R_a : 1.3 nm). Thermal (e, R_a : ca. 5.8 nm) and melt (f, R_a : ca. 2.4 nm) annealing seem to gradually removed (partially evaporated out) DIO. Scale bars in each image correspond to 2 μ m, Z (height)-scales are incorporated within each image.

Synthesis, DSC thermogram and NMR data

Monomer activation by Grignard synthesis: In a first flask, to a solution of 2-bromo-3-hexyl-5-iodothiophene (775 mg, 2.08 mmol) in 15 mL of dry THF under nitrogen atmosphere at RT was added *i*PrMgCl.LiCl (1.3 M solution in THF, 1.6 mL, 2.08 mmol). Mixture was stirred at room temperature for 1h. In a second flask, to a solution of 2-bromo-3-dodecyl-5-iodothiophene (950 mg, 2.08 mmol) in 15 mL of dry THF under nitrogen atmosphere at RT was added *i*PrMgCl.LiCl (1.3 M solution in THF, 1.6 mL, 2.08 mmol). Mixture was stirred at 40°C for 30 min then at RT for 30 more minutes. Copolymerization: Both Grignards were transferred onto a suspension of the catalyst Ni (dppp) Cl₂ (16 mg, 5.77.10⁻² mmol) in 1.4 mL of dry THF and resulting mixture was stirred overnight at RT. The polymerization solution was quenched with 10 mL of 5 M aqueous HCl and stirred for 30 min to stop the polymerization. The solution was poured in a large volume of cold methanol and the resulting precipitate was then filtered. Oligomers and impurities in the product were removed via Soxhlet extractions with methanol, acetone and hexane, followed by chloroform extraction. After reprecipitation the resulting solid was dried under vacuum to yield the copolymer ($M_n = 34$ kDa, PDI = 1.19) as a dark purple solid (590 mg, 68%). ¹H NMR (500 MHz, CDCl₃) $\delta = 6.98$ (s, H_{ar} and H_{ar}), 2.90-2.50 (m, Th-CH₂-C₅H₁₁ and Th-CH₂-C₁₁H₂₃), 1.8-1.6 (m, Th-CH₂-CH₂-C₄H₉ and Th-CH₂-CH₂-C₁₀H₂₁), 1.5-1.2 (m, Th-C₂H₄-C₃H₆-CH₃ and Th-C₂H₄-C₉H₁₈-CH₃), 0.92 (t, $J = 7$ Hz, C₅H₁₀-CH₃), 0.88 (t, $J = 7$ Hz, C₁₁H₂₂-CH₃). Ratio of hexyl/dodecyl 53/47, λ_{max} (CHCl₃) = 453 nm. ¹H-NMR spectrum was recorded in deuterated chloroform (CDCl₃) with 0.003% TMS (trimethylsilane) as an internal reference, on a Bruker AMX-500 apparatus at a frequency of 500 MHz. Estimation of the regioregularity is made on the peak at 2.81 by comparing the integral of the full signal to the one of the main peak corresponding to the repeating unit (**Figure S6b**). We can estimate the RR > 99% which is coherent with the synthetic procedure used. Size exclusion chromatography (SEC) was performed in THF at 35 °C using an Agilent liquid chromatograph equipped with an Agilent degasser, an isocratic HPLC pump (flow rate = 1 mL/min), an Agilent autosampler (loop volume = 100 μ L, solution conc. = 1 mg/mL), an Agilent-DRI refractive index detector and three columns: a PL gel 10 μ m guard column and two PL gel Mixed-D 10 μ m columns (linear columns for separation of MWPS ranging from 500 to 10⁷ g.mol⁻¹). Polystyrene standards were used for calibration. UV-Visible absorption spectrum of polymer solution was recorded in chloroform on a Cary UV-VIS 50 Varian spectrometer over a wavelength range of 300-800 nm. DSC

measurement was performed using a DSC Q200 from TA Instruments under nitrogen flow. Melting and crystallization temperatures of the polymer was evaluated through the following “heat/cool/heat” procedure: heating at 10 °C.min⁻¹ from -80°C to 250 °C, cooling at 5 °C.min⁻¹ to -80°C, heating at 10 °C.min⁻¹ to 250 °C. The first scan was to erase any prior thermal history of the sample. Tzero pans and lids were utilized and sample weight was 7.4 mg. See **Figure S6a** for DSC thermogram showing thermal phase transitions.

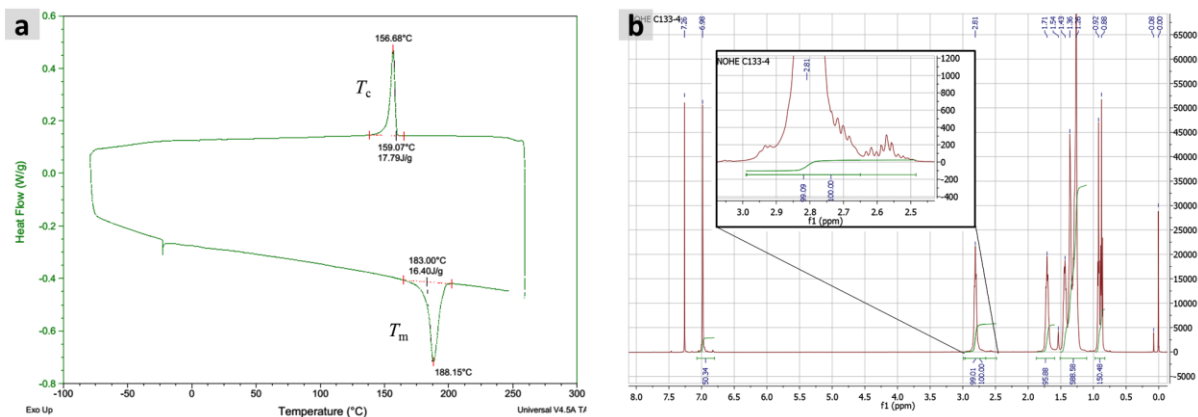


Figure S7: (a) DSC thermogram and (b) NMR data of P3HT-*co*-P3DDT we synthesized.

Calculation of free exciton bandwidth from absorption spectra of aggregated chains

The free exciton bandwidth (W) was calculated using Equation 4 in the main paper and the ratio A_{0-0}/A_{0-1} obtained from the absorption spectra of aggregated fraction. For the latter, the absorption spectra of aggregated fraction were fitted with a sum of Gaussian functions; see a representative example in **Figure S8**. The values are given in **Table S1**.

Table S1: The ratio A_{0-0}/A_{0-1} obtained from the absorption spectra of aggregated fraction and the free exciton bandwidth (W) is calculated using Equation 4 in the main paper. The error in A_{0-0}/A_{0-1} is $\pm 5\%$ and in W is $\pm 10\%$.

<i>Sample</i>	A_{0-0}/A_{0-1}	W (eV)
Neat as spin-coated	0.70 ± 0.04	0.097 ± 0.010
Neat_ T_{ca}	0.80 ± 0.04	0.061 ± 0.006
Neat_ T_{ma}	0.75 ± 0.04	0.079 ± 0.008
Neat_thin as spin-coated	0.73 ± 0.04	0.081 ± 0.008
Neat_thin_ SvA	0.94 ± 0.05	0.013 ± 0.001
+DIO as spin-coated	0.80 ± 0.04	0.062 ± 0.006
+DIO_ T_{ca}	0.91 ± 0.05	0.028 ± 0.003
+DIO_ T_{ma}	0.83 ± 0.04	0.053 ± 0.005
+DMDBS as spin-coated	0.69 ± 0.04	0.100 ± 0.010
+DMDBS_ T_{ca}	0.72 ± 0.04	0.092 ± 0.009
+DMDBS_ T_{ma}	0.78 ± 0.04	0.068 ± 0.007

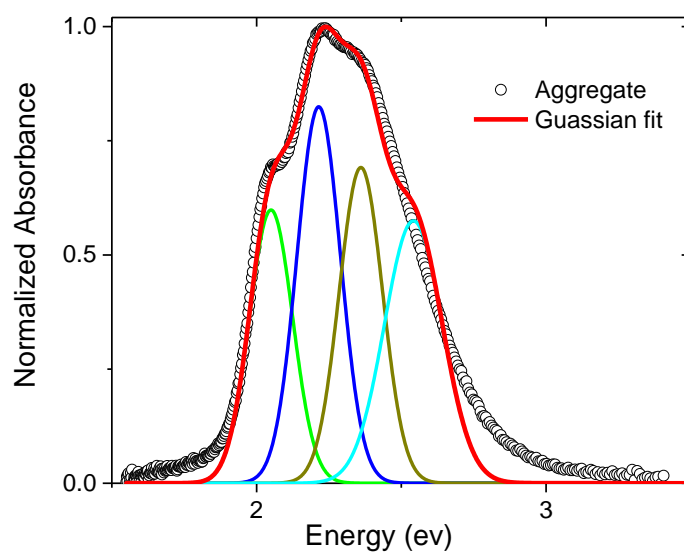


Figure S8: Fitting of the aggregate absorption spectra with a sum of four Gaussian functions. The width of the lower energy peaks was fixed, whereas it was allowed to vary for the fourth peak.